Chinese Chemical Letters 36 (2025) 109798

Contents lists available at ScienceDirect

Chinese Chemical Letters

journal homepage: www.elsevier.com/locate/cclet

Mechanism study of the molluscicide candidate PBQ on *Pomacea canaliculata* using a viscosity-sensitive fluorescent probe

Lanyun Zhang[a], Weisi Wang[b], Yu-Qiang Zhao[a], Rui Huang[a], Yuxun Lu[a], Ying Chen[b], Liping Duan[b,*], Ying Zhou[a,*]

[a] Yunnan Characteristic Plant Extraction Laboratory, College of Chemical Science and Technology, Yunnan University, Kunming 650091, China
[b] National Institute of Parasitic Diseases, Chinese Center for Disease Control and Prevention; Chinese Center for Tropical Diseases Research, WHO Centre for Tropical Diseases, National Key Laboratory of Intelligent Tracking and Forecasting for Infectious Diseases, Key Laboratory on Parasite and Vector Biology Ministry of Health, Shanghai 200025, China

ARTICLE INFO

Article history:
Received 30 January 2024
Revised 13 March 2024
Accepted 19 March 2024
Available online 20 March 2024

Keywords:
Fluorescence sensor
Viscosity
Pomacea canaliculata
Molluscicide mechanisms
Bio-imaging

ABSTRACT

PBQ [1-(4-chlorophenyl)-3-(pyridin-3-yl)urea], an enormous potent molluscicide, showed excellent *Pomacea canaliculata* (*P. canaliculata*) control activity and low toxicity for other aquatic organisms, but its snail-killing mechanisms are still not fully understood. We employed an optical method to elucidate PBQ action via a novel fluorescent viscosity probe, **NCV**. As the viscosity in the test solutions increased, compared with that in pure ethanol, a 54-fold fluorescence intensity enhancement of **NCV** was observed in 310 cP of 90% glycerol. Furthermore, **NCV** successfully exhibited a selective fluorescence response towards monensin-induced cellular viscosity changes in HepG2 cells. The liver, stomach, and foot plantar of the tested snails were frozen and sectioned for fluorescent imaging experiments after the treatment with different PBQ concentrations over various times. A significant fluorescent increase in the snail's liver was observed upon exposure to 0.75 mg/L PBQ for 72 h, which highlighted an increase in viscosity. Hematoxylin and eosin (HE) staining further supported PBQ-induced liver damage with a viscosity increase in *P. canaliculata*. Our study provides a new rapid optical visualization method to study the killing mechanisms of PBQ and may help discover new chemicals that control snail populations.

Pomacea canaliculata (Lamarck 1822), commonly known as the golden apple snail, is a freshwater snail native to South America and was introduced to China in the 1980s as a protein-rich food [1]. However, these snails were considered unpalatable [2], resulting in their neglect and invasion of southern China [3]. Currently, they are one of the top 100 worst invasive species in the world due to their rapid reproductive adaptability and lack of natural enemies. *P. canaliculata* favor aquatic plants as a food source, which can affect the structure and balance of plant communities in the aquatic environments they invade [4]. They are particularly partial to rice [5], making them a serious pest to rice seedlings [6]. Accordingly, there is an urgent need to implement effective control measures against *P. canaliculata* mitigation that can have a drastic influence on agricultural production.

According to reports, molluscicides for snails can usually be categorized into natural and synthetic products [7,8]. Several studies have described the molluscicide properties of certain plant extracts. Over the past five years, it was found that the alkaloid and saponin fractions extracted from *Tithonia diversifolia* exhibited high toxicity against *P. canaliculata* [9] and the molluscicidal activity of *Chimonanthus nitens* petroleum ether extracts on *Pomacea* snails 24 h half maximal inhibitory concentration (IC_{50}) was 0.287 mg/L [10]. Despite the advantages of high safety and environmental friendliness, the restricted yield and unstable effective extract levels significantly hinder their widespread application.

To date, chemical molluscicides have shown to be an effective strategy against invasive snails [11]. Nevertheless, most of the synthetic molluscicides lack selectivity and are environmentally hazardous [12,13]. As the only WHO-recommended molluscicide, 50% wettable powder of niclosamide methanolamine salt has been utilized as the only commercial chemical molluscicide in China for the last two decades [14]. However, this synthetic product has shown high toxicity towards 18 species of fish and other aquatic animals, which limits its application, particularly in aquaculture [15]. Hence, the development of molluscicides with a high level of molluscicidal activity and a low toxicity level to other organisms is extremely desirable.

* Corresponding authors
E-mail addresses: duanlp@nipd.chinacdc.cn (L. Duan), yingzhou@ynu.edu.cn (Y. Zhou).

https://doi.org/10.1016/j.cclet.2024.109798
1001-8417/

In 2018, we first [16] developed a series of pyridylphenylurea derivatives as molluscicide candidates against *B. straminea*, among them PBQ [1-(4-chlorophenyl)-3-(pyridin-3-yl)urea, also known as PPU07] showed good molluscicide activity in the laboratory. Then, we also evaluated PBQ molluscicida effectiveness in field trials against *Oncomelania hupensis* and toxicity to local fish [17]. In 2022, we continued to report that PBQ showed potent molluscicidal towards killing *P. canaliculate*, which exhibited the same quality molluscicidal effect with the niclosamide and slight toxicity towards other aquatic organisms [18]. Based on current findings, PBQ can be considered a highly efficient molluscicide with minimal environmental ramifications. However, it must be noted that there remains a lack of clear and in-depth research into the comprehensive understanding of its selective snail-killing mechanism.

Due to the various advantages of the fluorescence detection method, including high sensitivity, non-invasive character, high selectivity, and real-time imaging [19–22], we have developed novel methodologies for examining the killing mechanism of PPU-series compounds. In 2021, we reported a reaction-based near-infrared fluorescent probe (Niap) for the specific identification of alkaline phosphatase (ALP) with rapid red fluorescence enhancement. Our study revealed that PPU06 caused liver damage, resulting in snail death, and stimulated the increase of ALP in snails [23].

Moreover, the micro-environmental changes in live are more highly sensitive compared with enzyme level elevation for liver damage. In recent years, our research group has focused on viscosity as it is a key microenvironmental factor owing to its significant influence on many processes such as transport, signaling, and biomolecular interactions [24,25]. Over the past two years, we developed a mitochondrial targeting probe that can lead to tumor visualization and enable the study of the fluorescent visualization of nucleolar G-Quadruplex with an intranuclear viscosity probe [26,27].

Inspired by the above endeavors, herein, we aimed to design a novel viscosity-sensitive fluorescence molecule to investigate the viscosity changes in snails after PBQ treatment and to further explain the molluscicidal mechanism of PBQ with new optical ways. It is known that viscosity fluorescence sensors usually rely on molecular rotors [28]. In low-viscosity solvents, the molecular rotor is free to rotate, dissipate the excited state energy, and then increase the non-radiative transitions, ultimately leading to fluorescence quenching. While, in high-viscosity solvents, fluorescence enhancement can be achieved by simultaneously restricting the intramolecular rotation (RIR) and by the twisted intramolecular charge transfer (TICT) effect [28,29]. To track viscosity changes by intensity variations in fluorescence, a new rotator should be developed rationally based on this design strategy.

In the presented work, we designed a new rotator **NCV** by introducing a rotor to form TICT (Scheme 1), while integrating a robust electron-withdrawing group (benzaldehyde) and a potent electron-donating group (benzothiazole). After the treatment with PBQ, it showed that the strong orange fluorescence was mainly enriched in the liver of the snails and not in the stomach or foot plantar, which was the direct proof of the changes in viscosity. Additionally, hematoxylin and eosin (HE) staining further confirmed the liver damage. With the help of **NCV**, the test results showed that PBQ damaged the liver of golden apple snail, accompanied by increased viscosity in the microenvironment, which further led to snail death.

As shown in Scheme S1 (Supporting information), **NCV** was easily synthesized in a single step. The chemical structure of **NCV** was successfully confirmed by ^{1}H NMR and ^{13}C NMR spectroscopy, and high-resolution mass spectrometry (HRMS) (Figs. S1–S3 in Supporting information).

The spectral response of **NCV** to the viscosity was first measured in solution. The fluorescence emission spectra of probe **NCV**

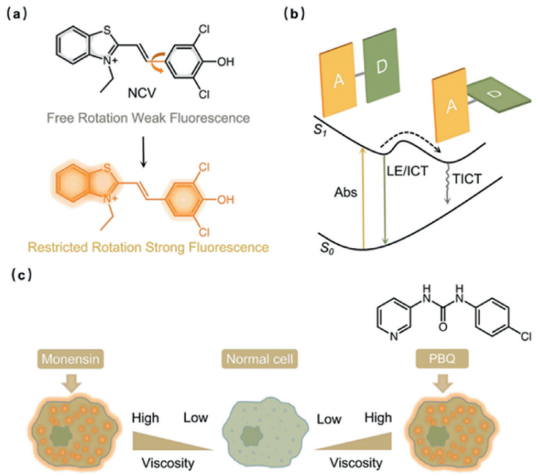

Scheme 1. (a) Molecular structure of **NCV**. (b) Viscosity sensing mechanism. (c) The illustration of viscosity changes in the cells induced by different endogenous stimulants.

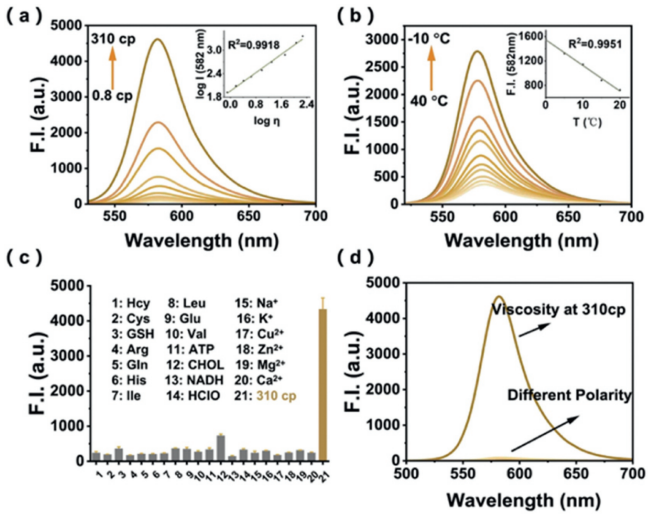

Fig. 1. (a) Fluorescence intensity of **NCV** (10 μmol/L) in phosphate buffered saline (PBS)-glycerol mixed solvents, insert: an image of the linear relationship between the log of maximum emission intensity of **NCV** at 582 nm (log I582) and log η (viscosity). λex = 470 nm, slits: 5/10 nm. (b) Fluorescence intensity changes of **NCV** (10 μmol/L) in different temperatures, insert an image of the linear relationship between I_{582} and temperature. (c) Fluorescence intensity of **NCV** (10 μmol/L) in PBS buffer (20 mmol/L, pH 7.4) with various species. (d) Fluorescence intensity changes of **NCV** in a 1,4-dioxane/water solvent system (10 μmol/L) in different polar solvents.

were measured, by adjusting different ratios of glycerol to ethanol, with viscosities ranging from 0.8 cP of pure ethanol to 310 cP of 90% glycerol (Table S1 in Supporting information). As shown in Fig. 1a, in low-viscosity solvents, **NCV** showed a weak emission intensity at 582 nm. As expected, the emission intensity was significantly enhanced as the viscosity of the solvent increased. An above 54-fold increase in fluorescence intensity (F.I.) was observed, with a good linear relationship that existed between log I_{582} (F.I. @582nm) and log η (viscosity) with a correlation coefficient of 0.9918. The obtained results indicated that **NCV** had a high viscosity sensitivity and could potentially be used for the quantitative measurement of viscosity.

To explore the effects of temperature on viscosity, the temperature of an ethanol-glycerol mixture (1:1, v/v) was regulated within the range of −10 °C and 40 °C, which resulted in temperature-dependent fluctuations in viscosity. The intensity of the emission peak at 582 nm showed a markable increase with decreasing tem-

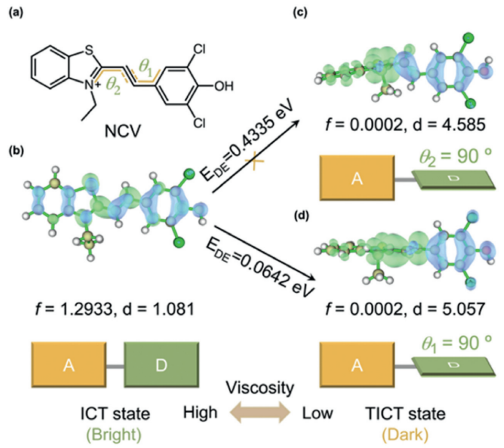

Fig. 2. (a) The molecular structure of **NCV**. (b) Schematic representation of the S_1 hole charge transition in the ICT state. (c) Schematic representation of the S_1 hole charge transition in the TICT state ($\theta_2 = 90°$). (d) Schematic representation of the S_1 hole charge transition in the TICT state ($\theta_1 = 90°$). Green and blue isosurfaces represent holes and charges, respectively.

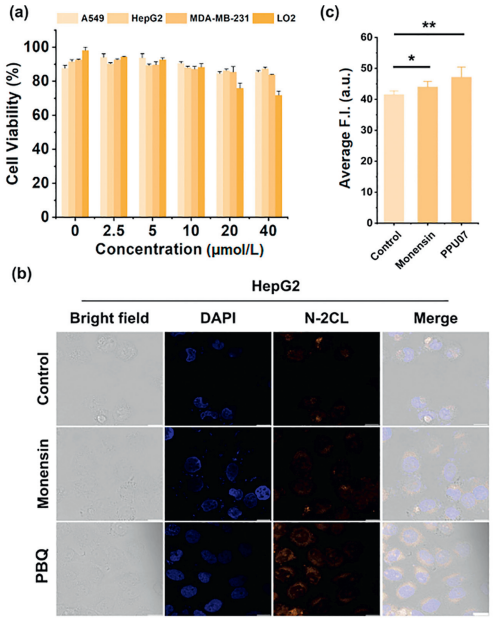

Fig. 3. (a) Cytotoxicity of **NCV** against various cell lines. Data were obtained using the standard MTS assay and cells were pretreated with different concentrations of **NCV**, bars denote the average of $n = 3$ measurements, while error bars denote the standard deviation. (b) Confocal fluorescence images of HepG2 cells. Group one: cells were incubated with **NCV** (10 μmol/L) for 15 min; group two: cells were pretreated with monensin (100 μmol/L) for 60 min and then incubated with **NCV** (10 μmol/L) for another 15 min, group three: cells were pretreated with PBQ (10 μmol/L) for 60 min and then incubated with **NCV** (10 μmol/L) for 15 min and 4,6-diamidino-2-phenylindole (DAPI, 10 μmol/L) for 30 min. Scale bar: 20 μm. (c) Average fluorescence intensity of each group of cells in panel (b). Bars denote the average of $n = 5$ measurements of random cells, while error bars denote the standard deviation. $^{*}P < 0.05$, $^{**}P < 0.01$, t test.

perature, as well as an excellent linear correlation ($R^2 = 0.9951$) (Fig. 1b). In addition, **NCV** absorbance at 582 nm in mixed solvents with varying ethanol to glycerol ratios displayed a consistent increased with increased viscosity (Table S1 in Supporting information). Meanwhile, with the viscosity of the solvent increased, the absorption intensity of **NCV** displayed a gradual decreasing trend, and a slight blue shift of the maximum absorption wavelength occurred. The absorption and the fluorescent spectra of **NCV,** in the range of pH 4–12, were shown in Figs. S4 and S5 (Supporting information).

To determine the interference toward **NCV,** some biologically relevant small molecules were monitored. The results are shown in Fig. 1c, where the potential interferents included homocystine (Hcy), cysteine (Cys), glutathione (GSH), arginase (Arg), glutamine (Gln), histidine (His), isoleucine (Ile), leucine (Leu), glutamate (Glu), valine (Val), asymmetric transport protocol (ATP), cholesterol (CHOL), nicotinamide adenine dinucleotide (NADH), HClO and some cations (Na^+, K^+, Cu^{2+}, Zn^{2+}, Mg^{2+}, Ca^{2+}). It showed that the fluorescent response of **NCV** towards high-viscosity was significantly stronger than that to the other tested potential factors.

According to reports, some viscosity sensors are sensitive to polarity, in which the signals can interfere with each other [19]. To investigate whether **NCV** suffered such an issue, the fluorescence response of **NCV** was measured at a constant viscosity while changing the polarity. Within the polarity range of all detected (Table S2 in Supporting information), only slight alterations in fluorescence were detected, as illustrated in Fig. 1d. The results showed that the signal stabilization of **NCV** was not affected by polar changes and can be used to test viscosity changes in a complex internal environment.

To gain deeper insight into the response mechanism of **NCV**, we conducted a detailed analysis of its structural characteristics. As illustrated in Fig. 2a, the benzothiazole moiety in **NCV** served as an electron acceptor, and the dichlorophenol functioned as an electron donor with the centrally positioned *trans*-double bond acting as a π-bridge to link the donor-acceptor (D-A) structure. The hole charge analysis of the first excited state (S_1) (Fig. 2b) further highlighted that dichlorophenol predominantly served as the major electron donor, while the benzothiophene moiety played a primary role as the electron acceptor [30–32]. Importantly, the presence of two dihedral angles in **NCV** molecules is susceptible to rotation (θ_1 and θ_2, as depicted in Fig. 2a). To validate the occurrence of TICT, we conducted calculations for two conformations with $\theta_1 \approx 90°$ and $\theta_2 \approx 90°$, respectively. In comparison to the planar conformation (intramolecular charge transfer (ICT) state, where θ_1 and θ_2 were both less than approximately 6°), the oscillator strength (f) of the first excited state (S_1) for the two perpendicular conformations was markedly less than 0.01. Moreover, these conformations exhibited evident hole-charge separation characteristics, with a charge transfer distance (d_{CT}) surpassing 4.59 Å (Fig. 2c), indicating they were representative of the TICT state. Notably, TICT state with $\theta_2 \approx 90°$ exhibited a higher energy level, which was less conducive to the manifestation of TICT. Conversely, TICT state with $\theta_1 \approx 90°$ boasts an energy level in proximity to the ICT state (Fig. 2d). Hence, θ_1 played a dominant role in driving the TICT process. In the case of a different rotatable angle, it possesses the potential to engage in the non-radiative relaxation process of the excited state through rotational energy consumption. As previously indicated, within an unrestrained microenvironment, the rotor of **NCV** undergoes either passage through its rotational motion, resulting in non-radiative relaxation of the excited state energy, or entry into the dark state of TICT, culminating in a weak fluorescence emission. However, in a high-viscosity environment, the intramolecular rotation is notably impeded, thereby diminishing the likelihood of non-radiative transitions and the TICT state. This inhibition ultimately promotes changes in the fluorescence. Consequently, the viscosity sensitivity of **NCV** was a distinctive feature attributed to the behavior of its rotor.

Furthermore, the cytotoxicity of **NCV** was evaluated in various living cell lines, including cancer cells (A549, HepG2, and MDA-MB-231 cells) and normal human cells (LO2 cells). The conventional MTT assay demonstrated that **NCV** did not exhibit significant cytotoxic effects on cells at different micromolar concentra-

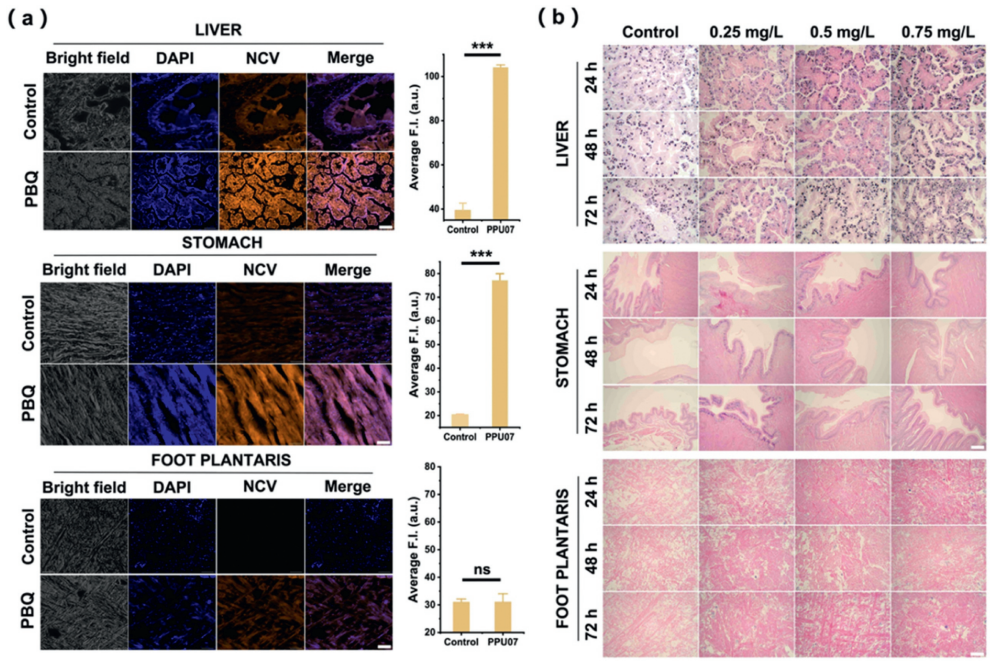

Fig. 4. (a) Left: The fluorescence imaging of liver, stomach, and foot plantar slices from *P. canaliculate*, after 72 h PBQ (0.75 mg/L) incubation. Blue channel: DAPI (10 μmol/L) for 30 min; orange channel: NCV (20 μmol/L) for 15 min. Right: average fluorescence intensity of each group of slices in panel (a), bars denote the average of $n = 5$ measurements of random cells, while error bars denote the standard deviation. $^{***}P < 0.001$, t test. (b) After incubation with different PBQ concentrations for varying treatment time, histopathologic slides with HE staining from the liver, stomach, and foot of *P. canaliculate*. Scale bar: 60 μm.

tions (Fig. 3a), as well as highlighting its potential for further cell imaging.

To determine the effect of PBQ on cell viscosity during snail killing, monensin was chosen as the endogenous stimulus to increase the intracellular viscosity by causing structural changes or swelling of mitochondria [33]. Owing to **NCV**'s ability to act as an efficient tool for the detection of intracellular viscosity, a distinct fluorescence of **NCV** was observed in HepG2 cells, after treatment with 10 μmol/L monensin for 1 h and then incubated with **NCV** (10 μmol/L) for 15 min (Fig. 3b). The control group showed insignificant fluorescence emission. These findings confirmed the successful fluorescence response and selectivity of **NCV** for cellular viscosity measurement. Next, HepG2 cells were pretreated with 10 μmol/L PBQ under the same conditions, resulting in a strong orange fluorescence by **NCV** (Fig. 3c). Therefore, the action of PBQ could induce changes in the intracellular viscosity.

Following PBQ treatment, **NCV** was utilized to detect the viscosity of the snails' organs. *P. canaliculata* were collected from Dali City, Yunnan Province, China (25.71 °N, 100.1 °E) and kept for one week in plastic containers filled with a specified volume of fresh water to allow them to acclimatize to laboratory conditions and scientific feeding. Ten groups of 60 adult *P. canaliculata* ($n = 6$, per group) were placed in suspensions (400 mL) of PBQ at varying concentrations (0, 0.25, 0.5, and 0.75 mg/L). The experiments were performed within a temperature range of 22–26 °C and each concentration was repeated in triplicate. The surviving snails were randomly selected from test groups after 24, 48, and 72 h of exposure. The shells of the tested snails were shattered, and their liver, stomach, and foot plantaris were processed and prepared for the next two methods, including frozen tissue sections and HE staining experiments.

The fluorescence imaging experiments on frozen sections were performed to detect the effects of PBQ on the viscosity of snail organs. In the control group (0 mg/L PBQ), a weak orange fluorescence was observed in the liver and stomach, which indicated the intrinsic viscosity of normal snail livers and stomachs. However, as PBQ concentration increased, the orange fluorescence enhanced in the liver and stomach, reaching a maximum at 0.75 mg/L PBQ after 72 h. There was no distinct change in the intensity of the plantar foot in the test group (Fig. 4a). The results showed that PBQ was probably acting on the liver and stomach and that the viscosity of both organs increased significantly upon exposure to PBQ.

To further confirm organ damage, HE staining was used to observe the tissue structure of *P. canaliculata* organs, including the liver, stomach, and foot (Fig. 4b and Figs. S6–S8 in Supporting information). The control group's tubules of the digestive glands of the liver were intact, and no abnormalities were detected. The lesions caused by different PBQ concentrations and treatment times showed a positive gradient change. Only slight damage was observed at 0.25 mg/L with 24 h treatment, the digestive gland tubules of the liver began to dissolve, and the serosa was thinner than that of the control group. However, as the drug concentration and immersion time increased, the liver damage became more pronounced. After exposure to 0.5 mg/L **NCV** for 72 h, the digestive tubules of the liver were noticeably dissolved, and the tissue structure was incomplete. When the immersion concentration reached 0.75 mg/L for 72 h, *P. canaliculata* was severely damaged, digestive gland tubules and crypta of the liver were dissolved and large areas of necrosis occurred in the liver. In addition, the findings of HE showed that the villous epithelium of the stomach of the control group was intact. With increasing concentration and duration, the villous epithelium of the stomach was gradually dissolved. Besides, no significant pathological changes were observed in foot sections. It proved that PBQ mainly acted and caused serious damage on the liver.

To study the injury effects in the liver and stomach of *P. canaliculate*, we incubated the snails with different concentration of PBQ for various time. As shown in the florescent experiments (Figs. 5a and b), there was a positive correlation between fluorescence

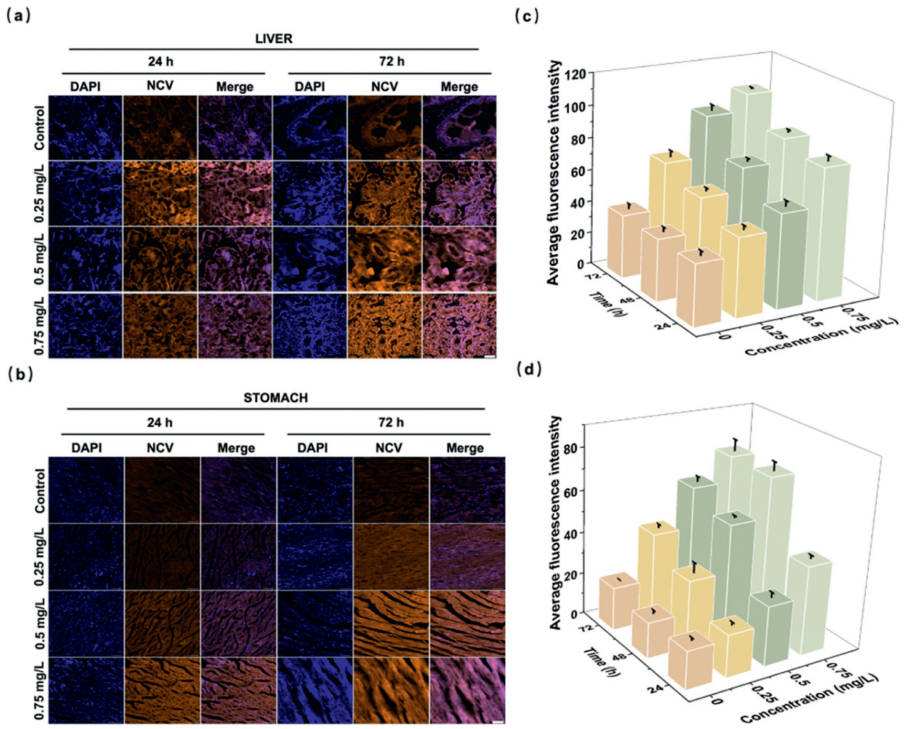

Fig. 5. (a, b) The slices of the liver and stomach of *P. canaliculata*, which were incubated with a PBQ concentration of 0, 0.25, 0.5, and 0.75 mg/L for 24 h and 72 h, incubated with 20 μmol/L **NCV** for 15 min and DAPI (10 μmol/L) for 30 min. The section thickness was 10 μm, scale bar was 60 μm. (c, d) Average fluorescence intensity of each group of the slices of liver and stomach.

intensity and concentration of PBQ, ranging from 0.25 mg/L to 0.75 mg/L. Through the fluorescence intensity changes, it showed the damage effects of PBQ to liver and stomach reached a maximun at 0.75 mg/L in 72 h (Figs. 5c and d). In the tested concentration of PBQ, as the orange fluorescence in liver was always apparently stronger than that in stomach, these results provided further strong evidence, that the PBQ mainly affected the liver.

In summary, we designed and produced a novel viscosity-sensitive compound **NCV** as a fluorescent tool to further explain the molluscicidal mechanism of PBQ in *P. canaliculata*. **NCV** was found to be highly sensitive towards viscosity, and the detection of changes was possible with minimal interference from polarity and other biologically related species. The results of the fluorescence imaging showed that **NCV** could successfully generate the selective fluorescent response to the cellular viscosity changes induced by monensin in HepG2 cells. After exposure to various concentrations and treatment times of PBQ, the frozen tissue of three kinds of organs form golden apple snails were obtained. The fluorescent results demonstrated that the viscosity of the liver increased significantly compared to that of the stomach and foot plantar after treatment. HE staining confirmed that PBQ caused severe liver damage. The utilization of **NCV** revealed that PBQ mainly stimulated an increase in viscosity in the snail's liver and caused heavy liver damage, leading to snail death. In this study, we provided a new rapid optical visualization method to study the killing mechanism of PBQ, which may facilitate the development of additional molluscicides.

Declaration of competing interest

The authors declare that they have no known competing financial interests or personal relationships that could have appeared to influence the work reported in this paper.

Acknowledgments

The authors are indebted for the financial support of this work by the National Natural Science Foundation of China (Nos. 82072309, 22067019 and 22367023), the Major Science and Technology Projects in Yunnan Province (No. 202402AE090006), the Project of Yunnan Characteristic Plant Screening and R&D Service CXO Platform (No. 2022YKZY001), Yunnan Provincial Science and Technology Department Yunnan University Joint Special Project (No. 202201BF070001-001), the Postgraduate Research Innovation Foundation of Yunnan University (No. KC-23234403), the Scientific Research Foundation Project of Yunnan Provincial Department of Education (No. 2023Y0240).

Supplementary materials

Supplementary material associated with this article can be found, in the online version, at doi:10.1016/j.cclet.2024.109798.

References

[1] R.H. Cowie, Apple snails (Ampullariidae) as agricultural pests: Their biology, impacts and management, in: GM Baker (Ed.), Molluscs as Crop Pests, CABI Publishing, Wallingford, 2002, pp. 145–192.
[2] X. Zhou, Y. Chen, S. Zhu, et al., Mitochondr, DNA Part A 27 (2016) 884–885.
[3] T. Wada, K. Matsukura, J. Molluscan Stud. 77 (2011) 149–153.
[4] M. Halwart, Int. J. Pest Manage. 40 (1994) 199–206.
[5] K. Matsukura, K. Yoshida, Hydrobiologia 851 (2024) 195–203.
[6] G.M. Luque, C. Bellard, C. Bertelsmeier, et al., Biol. Invasions. 16 (2014) 981–985.
[7] C.P. Yang, Y.M. Wang, Y.Q. Ma, et al., Ecotoxicol. Environ. Saf. 246 (2022) 114198.
[8] G.J. Yang, W. Li, L.P. Sun, et al., Parasit. Vectors 3 (2010) 84–92.
[9] K.A. Ballada, Z.G. Baoanan, Environ. Dev. Sustain. (2023), doi:10.1007/s10668-023-03969-5.
[10] S. Li, Z. Zou, Pestic. Biochem. Physiol. 160 (2019) 136–145.
[11] X.Y. Wu, L.Q. Yang, L.H. Zhang, et al., Chin. J. Schisto. Control 18 (2006) 474–476.

[12] N.M.F. Lima, A.F.D. Santos, Z. PorfiñRio, et al., Acta Trop. 83 (2002) 43–47.
[13] X.H. Liu, X.Y. Xu, C.X. Tan, et al., Pest. Manage. Sci. 71 (2015) 292–301.
[14] Y. Yuan, X.J. Xu, H.F. Dong, et al., Acta Trop. 96 (2005) 191–197.
[15] T. Osada, M. Chen, X.Y. Yang, et al., Cancer Res. 71 (2011) 4172–4182.
[16] W. Wang, Q. Mao, J. Yao, et al., Parasit. Vectors 11 (2018) 291–298.
[17] Z. Chen, W. Wang, J. Yao, et al., Chemosphere 222 (2019) 56–61.
[18] W. Wang, S. Huang, F. Liu, et al., J. Agric. Food Chem. 70 (2022) 1079–1089.
[19] X. Yang, D. Zhang, Y. Ye, et al., Coord. Chem. Rev. 453 (2022) 214336.
[20] Y. Lu, J. Xu, Z. Jia, et al., Chin. Chem. Lett. 33 (2022) 1589–1594.
[21] S. Cai, L. Wu, Y. Li, et al., Chin. Chem. Lett. 35 (2024) 108599.
[22] Z. Li, Q. Qiao, N. Xu, et al., Chin. Chem. Lett. 35 (2024) 108824.
[23] C. Liu, S. Yang, Y. Qiao, et al., Chin. Chem. Lett. 32 (2021) 1809–1813.
[24] M. Ren, Q. Xu, S. Wang, et al., Chem. Commun. 56 (2020) 13351–13354.
[25] Y. Zhou, P. Li, X. Wang, et al., Chem. Sci. 11 (2020) 12149–12156.
[26] L. Yu, P. Verwilst, I. Shim, et al., CCS Chem. 3 (2021) 2725–2739.
[27] L. Yu, J.F. Zhang, M. Li, et al., Chem. Commun. 56 (2020) 6684–6687.
[28] M.A. Haidekker, E.A. Theodorakis, Org. Biomol. Chem. 5 (2007) 1669–1678.
[29] C. Wang, W. Chi, Q. Qiao, et al., Chem. Soc. Rev. 50 (2021) 12656–12678.
[30] T. Lu, F. Chen, J. Comput. Chem. 33 (2012) 580–592.
[31] Z. Liu, T. Lu, Q. Chen, Carbon. 165 (2020) 461–467.
[32] M.J. Frisch, G.W. Trucks, H.B. Schlegel, et al., Gaussian 09, Revision E.01, Gaussian, Inc., Wallingford, CT, 2013.
[33] H. Wang, M. Dong, H. Wang, et al., Chem. Commun. 57 (2021) 5838–5841.